Naval Research Laboratory
Washington, DC 20375-5320

NRL/MR/6410--00-8507

Advanced Simulation Tool for Improved Damage Assessment 2) Water-Mist Suppression of Large Scale Compartment Fires

KULDEEP PRASAD*
GOPAL PATNAIK
K. KAILASANATH

Center for Reactive Flow and Dynamical Systems
Laboratory for Computational Physics and Fluid Dynamics

**Science Applications International Corporation, VA*

December 29, 2000

REPORT DOCUMENTATION PAGE

Form Approved
OMB No. 0704-0188

1. AGENCY USE ONLY (*Leave Blank*)	2. REPORT DATE	3. REPORT TYPE AND DATES COVERED
	December 29, 2000	NRL Memorandum Report

4. TITLE AND SUBTITLE

Advanced Simulation Tool for Improved Damage Assessment
2) Water-Mist Suppression of Large Scale Compartment Fires

5. FUNDING NUMBERS

6. AUTHOR(S)

Kuldeep Prasad,* Gopal Patnaik, and K. Kailasanath

7. PERFORMING ORGANIZATION NAME(S) AND ADDRESS(ES)

Naval Research Laboratory
Washington, DC 20375-5320

8. PERFORMING ORGANIZATION REPORT NUMBER

NRL/MR/6410--00-8507

9. SPONSORING/MONITORING AGENCY NAME(S) AND ADDRESS(ES)

Office of Naval Research
800 N. Qunicy Street
Arlington, VA 22217-5660

10. SPONSORING/MONITORING AGENCY REPORT NUMBER

11. SUPPLEMENTARY NOTES

*Science Application International Corporation, VA

12a. DISTRIBUTION/AVAILABILITY STATEMENT

Approved for public release; distribution is unlimited.

12b. DISTRIBUTION CODE

13. ABSTRACT (*Maximum 200 words*)

This report is the second in a series that discusses the development of an advanced simulation tool for improved damage assessment. In the first report, we adopted a domain decomposition approach, based on the multiblock Chimera technique, to simulate fires in single uncluttered compartments and predicted spread of smoke in multicompartment ship geometries. These simulations demonstrated the capability of the tool to simulate complex flow fields in large multicompartment enclosures.

In this report, we focus on simulating water-mist suppression of fires in large enclosures. A two-continuum formulation is used in which the gas phase and the water-mist are both described by equations of the Eulerian form. The water-mist model is coupled with previously developed codes based on the multiblock Chimera technique for simulating fires. Computations are now performed to understand the various physical processes that occur during the interaction of water-mist and fires in large enclosures. Droplet sectional density contours and velocity vectors are used to track the movement of water-mist and to identify the regions of the fire compartment where the droplets evaporate and absorb energy. Parametric studies are performed to optimize various water-mist injection characteristics for maximum suppression. The effects of droplet diameter, mist injection velocity, injection density, nozzle locations and injection orientation on mist entrainment and flame suppression are quantified. Numerical results indicate that for similar injection parameters such as mist injection density, injection velocity and droplet diameter, the time for suppression was smallest for the top injection configuration. Water-mist injection through the side walls, the front and rear walls, and the floor were found to be less efficient than the top injection configuration. These results are compared with our earlier predictions on water-mist suppression of small-scale methanol pool fires and other experimental studies.

14. SUBJECT TERMS

Fire suppression
Compartment fires
Multiblock techniques

15. NUMBER OF PAGES

27

16. PRICE CODE

17. SECURITY CLASSIFICATION OF REPORT	18. SECURITY CLASSIFICATION OF THIS PAGE	19. SECURITY CLASSIFICATION OF ABSTRACT	20. LIMITATION OF ABSTRACT
UNCLASSIFIED	UNCLASSIFIED	UNCLASSIFIED	UL

CONTENTS

LIST OF FIGURES

LIST OF TABLES

Advanced Simulation Tool for Improved Damage Assessment. 2) Water-mist Suppression of Large Scale Compartment Fires

1. INTRODUCTION

This report is the second in a series that discusses the development of an advanced simulation tool for improved damage assessment. In the first report, we described a multiblock technique to simulate the reactive fluid flow inside large complex enclosures. We adopted a domain decomposition method, based on the multiblock Chimera technique, which allows a system of relatively simple grids, each describing a component of the complex geometry, to be combined into a composite mesh for solution to complex flow fields. Using this approach we studied fires in a single uncluttered compartment and predicted smoke spread in multi-compartment ship geometries. These simulations demonstrated the capability of the tool to simulate complex flow fields in large multi-compartment enclosures. In this report we focus on the suppression of fires in large compartments and conduct parametric studies to optimize various water mist injection characteristics for maximum fire suppression.

Fine water mist relies on relatively small (less than 200 μm) droplet sprays to extinguish fires. For optimum use of water mist systems, the various physical processes involved in the interaction of water mist spray and the fire should be clearly understood. Typically, water mist is injected through various strategically located nozzles into a fire compartment. The turbulent flow field in the fire compartment may consist of a fire plume consisting of hot combustion products rising above the fuel source. The fire plume hits the ceiling and spreads along the ceiling. Vortical structures are continuously generated as fresh air is entrained into the fire. The flow of water droplets through such a hot turbulent environment should be understood. Besides there might be actual physical barriers or obstructions in the fire compartment that may prevent water mist from reaching the fire source. Once the water mist starts interacting with the fire source, the mechanism of fire suppression may include gas phase cooling (thermal effect), oxygen displacement by steam, wetting of fuel surface and attenuation of radiative heat transfer. Efforts to explain the mechanisms of extinguishment of fire, and to identify the parameters that are crucial to system design, benefit greatly from the application of computational models to simulate the dynamics of fires. Research [1] indicates that the relationship between spray characteristics, fuel properties, compartment geometry and the probability of extinguishment is a multi-variable problem that can best be analyzed using computational models. This report describes numerical simulations of water-mist suppression of fires in large complex enclosures, to better understand and probe these issues.

The available research in water spray fire extinguishment was reviewed by Rashbash [2] and by

Manuscript approved December 9, 2000.

Tatem et al. [3]. There is vast body of literature that covers the area of small flames and suppression of laboratory scale fires. This includes experimental and numerical studies involving counterflow and co-flow configurations and laboratory scale premixed and diffusion flames. We have reviewed this work extensively in previous journal articles and reports [4]- [10]. We have chosen not to discuss this portion of the literature again, since the focus of this report is on fire suppression in large compartments and in multi-compartment enclosures.

Water as a means of fire suppression has been in use from ancient times. The phase-out of halons and the need for efficient sprinkler systems on commercial ships has sparked a renewed interest in understanding the dynamics of water-mist suppression of fires in large compartments or in multi-compartment enclosures. Downie et al. [11] has studied the suppression of a large methane fire subjected to a steady water mist spray from a single hollow cone nozzle mounted above the fire. The large plume to flame thrust ratio in their experiment resulted in negligible direct penetration of the droplets into the fire region. Their result shows a significant reduction in oxygen concentration and increase in carbon monoxide concentration inside the flame when the mist was applied. Mawhinney [12] has adopted a "first principles" approach to the design of water-mist systems. Using a commercially available CFD model TASCflow, he showed that fire extinction in large compartments is a function of fuel properties, spray characteristics, details of application and methods of fire detection and system activation. Mawhinney [13] has also discussed the relative importance of various fire suppression mechanisms, such as heat extraction, oxygen displacement and radiant heat attenuation. A detail understanding of these mechanisms is critical in designing a suppression system for a particular fire scenario and in development of computer models for studying water-mist suppression systems. Ndubizu et al. [14] have performed an experimental parametric study of water-mist suppression of large-scale liquid pool fires. They have investigated the effects of droplet size and injection orientation on water-mist suppression of low and high boiling point liquid pool fires. The results of their study were compared with numerical studies on small scale methanol pool fires [15,16].

A series of fire tests was conducted by the National Institute of Standards and Technology [17] in several typical office occupancy configurations in order to address the use of quick response sprinkler technology. These tests included 1) heat release rate tests, 2) compartment fire tests and 3) a large office test. The compartment fire tests were designed to examine the effectiveness of quick response sprinklers in typical office fires involving a computer work station or an open office module. The large office test configured with multiple open office modules was conducted to verify the compartment test results and examine the possibility of multiple sprinkler activation. Cooper and Stroup [18] have analyzed a portion of the data acquired during these tests to study the effects of elevated temperatures in the upper smoke layer and its impact on the thermal response of sprinkler links.

Recently several numerical studies [19]- [25] have been conducted to simulate the suppression of fires in large uncluttered compartments. Alpert [19] developed a field model to predict the penetration of a sprinkler spray through the plume of a burning object. The model essentially combines a model of a 2-D flow produced by a plume of a heated jet and a water spray model. Later, the model was verified using the Factory Mutual Research Corporation's actual delivered density (ADD) apparatus [20]. Their results show some good agreement between the predicted and measured density of water reaching the base of a heptane spray fire when the sprinkler nozzles are located 3.05 m and 4.57 m above the base. The dynamics of highly sooting fires in unbounded

domains have been investigated by Mell et al. [21]. McGratten and Stroup [22] have numerically investigated conditions under which vents and draft curtains are beneficial, and under which they are detrimental, to the performance of a sprinkler system in large enclosures. Parametric studies [23] have been performed to predict the actual delivered densities of early suppression fast response sprinklers in heptane spray fire scenarios. Hoffman and Galea [24,25] developed another field model of a compartment fire with the sprinklers turned on. The predictions of the model were later verified with experimental data for a corner fire in an office size compartment as well as a bed fire in a large hospital room. The temperature predictions in both cases were (qualitatively) in good agreement with experimental results.

Over the past five years, we have done a significant amount of work [4]- [10], in understanding the interaction of water-mist with methane air diffusion flames and liquid methanol pool fires. A numerical model [4,5] was developed to study the suppression of gas jet diffusion flames using water droplets. A two-continuum formulation was used in which the gas phase and the water-mist are both described by equations of the eulerian form. The model was used to obtain a detailed understanding of the physical processes involved during the interaction of water mist and flames. The relative contribution of various mist suppression mechanisms was studied. Next, a numerical study was conducted to optimize various water mist injection characteristics for maximum flame suppression. The effects of droplet diameter, mist injection angle (throw angle), mist density and velocity on water-mist entrainment into the flame and flame suppression were quantified [6,7]. A liquid methanol pool model was then developed and coupled with the gas phase combustion to describe the burning of a pool of liquid methanol [8,16]. The models were again extended to study the effect of water-mist on pool burning rate, flame suppression and extinction [9,15]. Although this research is very useful in understanding the detailed interaction of water-mist and fires, it was limited to small scale pool fires. In practical Navy applications much larger fires are encountered in complex ship geometries. There was clearly a need to develop a model for studying fires in large enclosures. The authors have developed a multiblock domain decomposition technique based on the "CHIMERA" approach [26] to solve the unsteady compressible Navier Stokes equations inside a large fire compartment. Computations [10] were performed to demonstrate seamless fluid flow through three embedded grids. Simulations were performed for a 980 kW fire in a single uncluttered compartment as well as for a 1310 kW fire in multi-compartment ship geometry (ex-USS Shadwell) [10].

In this report we extend the study to investigate the effect of water-mist on fire suppression in large complex enclosures. An Eulerian water-mist sectional model is combined with the gas phase equations for studying water mist interaction with large fires. The two-continuum model is used to study mist entrainment into the fire and to predict the time required for extinction of the fires. A parametric study is also described in which the effect of various water-mist injection characteristics such as drop diameter, injection density, velocity, nozzle orientation and location on overall fire suppression is investigated. The results of this study are compared and contrasted with previous observations with small scale methanol pool fires and other experimental studies.

2. MATHEMATICAL AND NUMERICAL FORMULATION

Several recent developments in computational techniques have been combined to develop a tool that can be used to simulate fires in large complex enclosures, the interaction of water-mist with these fires, entrainment of water-mist and overall fire suppression and extinction. Many of these

techniques have been discussed extensively in earlier reports and papers [4]- [10]. We have adopted a method of domain decomposition based on the multiblock "CHIMERA" approach [26] which allows a system of relatively simple grids, each describing a component of the complex geometry, to be combined into a composite grid to yield solutions for complex flow fields. The domain decomposition technique subdivides the entire computational region into several smaller blocks. The Chimera approach [10] requires that adjacent blocks overlap each other in a way that flow field information can be exchanged. Independent blocks communicate flow field information with adjacent blocks through a system of artificial boundaries also known as interpolation boundaries and hole creation boundaries. Fractional time step splitting techniques are used not only for the physical processes but also to couple the solutions for the individual blocks. The multiblock technique has been found to be very suitable for simulating fire growth through single uncluttered compartment and for studying smoke spread in large multi-compartment enclosures [10].

The complete set of unsteady compressible Navier Stokes equations are solved in the entire fire compartment [4,5,10]. Chemical reactions between the fuel and the oxidizer species are studied using single step kinetics [4,6]. These chemical reactions are allowed to occur only in the blocks that surround the individual fires and the fuel sources [10]. In a typical fire compartment, water-mist is injected through nozzles that are located strategically at various positions for optimum fire suppression. At any given time, there could be millions of water-droplets in the fire compartment. It is computationally not feasible to track the size and spatial location of each and every droplet in the fire compartment. We have adopted a sectional water-mist model [5,7], in which the entire droplet size domain is divided into discrete sections, and track only one integral quantity within each section. The advantage of this approach is that the integral quantity is conserved and the number of equations is significantly reduced to be equal to the number of sections. This results in a two-continuum formulation, wherein the gas properties and the droplet properties are each described by equations in the Eulerian form. Each of the droplet sections is assumed to have its own unique velocity different from that of the gas phase. Momentum conservation equations are formulated for each droplet section and are coupled to those of the gas phase through the phase interaction terms (drag terms).

The governing equations are rewritten in terms of finite-volume approximations on an Eulerian mesh and solved numerically for specific boundary and initial conditions. A complete solution to these governing equations require solving the terms for each of the individual processes, as well as accounting for the interaction among the processes. The solution approach consists of separate algorithms for each of the individual processes, which are then coupled together by the method of time-step splitting. The algorithms for convection, thermal conduction, molecular diffusion, viscosity and the coupling of the individual processes have been previously discussed in detail [27].

The fluid convection is solved with a high-order implicit algorithm, Barely Implicit Correction to the Flux-Corrected Transport (BIC-FCT) [27]. that was developed to solve the convection equations for low-velocity flows. The Flux-Corrected Transport (FCT) [28] algorithm itself is an explicit, finite-difference algorithm that is constructed to have fourth-order phase accuracy. Through a two-step predictor-corrector algorithm, FCT ensures that all conserved quantities remain monotone and positive. The solution of three-dimensional reactive flow equations on a large number of grid points is a challenging computational task. The presence of water-mist introduces additional conservation equations that have to be solved along with conservations equations for mass, momentum and energy. In this code, explicit shared memory directives using the OpenMP standard were placed

strategically to ensure large regions of the code will operate in parallel. The combined choice of Fortran 90 and OpenMP allows this code to be ported to a variety of computers, but it is best suited to shared memory computers such as the Cray C-90 and or the SGI Origin 2000.

3. RESULTS AND DISCUSSION

Dembsey, Pagni and Williamson [29] have performed a set of full-scale compartment fire experiments suitable for model comparison. The experiments were conducted in a fire test compartment (Figure 1) which is 2.5×3.7 m in plan and 2.5 m in height. The compartment is similar in size, geometry and construction to the standard fire test compartment specified in Uniform Building Code Standard 8-2. A 0.61 $m\times$ 1.22 m porous surface burner was placed in the center of the compartment. The burners porous surface was 0.61 m above the floor of the compartment. Propane fuel was supplied at a steady rate to obtain a 330 kW or 980 kW fire for the duration of each experiment. As shown in Figure 1, the ceiling gas temperature distribution was measured using fifteen thermocouples arranged in a uniform grid centered in the compartment, 0.10 m below the ceiling. The compartment has a single doorway, 0.76 m wide $\times$2.0 m high centered on one of the shorter sides.

In an earlier report [10], we had described results of numerical simulations in a geometry similar to the one used by Dembsey, Pagni and Williamson. The fire compartment was gridded with a $36 \times 24 \times 24$ cartesian mesh with a uniform gridding of 10.0 cm. The burner and the fire were gridded relatively finely using a $32 \times 24 \times 24$ cartesian mesh embedded within the fire compartment mesh. The fire compartment was connected through the door to a very huge compartment referred to as the "outer compartment". The outer compartment was gridded with a $64 \times 48 \times 72$ mesh. The presence of the outer compartment does not appreciably increase the cost of the calculations, but it provides a reasonable way of computing the flow field through the door. The door became an interior plane of the computational domain and not a boundary condition. Simulations were performed for a 330 kW and a 980 kW fire located in the center of the compartment. The fire was ignited at $t = 0$ s and the simulations were terminated at $t = 1800$ s. Numerical results for the ceiling gas temperature distribution were found to compare favorably with experimental data recorded at fifteen thermocouples located 0.1 m below the ceiling [10].

In this paper, the earlier study is extended to simulate water mist suppression of this fire. Numerous simulations were performed to investigate the effect of various water mist injection parameters, such as drop diameter, injection velocity, injection density, nozzle orientation and location of the nozzle on overall fire suppression and extinction.

We first describe one specific simulation in which water mist was injected through four nozzles located in the ceiling and were directed vertically downward toward the fire. The nozzles are centered around the co-ordinate location $(70, 250, 70)$, $(70, 250, 170)$, $(300, 250, 70)$ and $(300, 250, 170)$ cm (see Figures 2-4 for the co-ordinate system). Water mist is injected vertically downward with an injection velocity of 100.0 cm/s and an injection density of 0.2 gm/cm^3. The injected droplets are monodisperse with an initial droplet diameter of 100 μm. This results in a total mist flow rate of 200 kg/s. The entire droplet domain consists of one section only ranging from $0 - 100$ μm. As in the earlier report [10], a 980 kW fire is ignited at $t = 0$ s and is allowed to develop fully till time $t = 1800$ s. At this time the water mist is injected through the four nozzles.

Figure 2 shows the water-mist sectional velocity vectors superimposed on a surface temperature

plot for a 980 kW fire. The length of the arrows indicates a magnitude of the velocity vectors and the vectors point in the direction of the local mist flow. The velocity vectors indicate that water mist that is injected vertically downward, quickly changes direction and tends to flow along with the air flow. Water-mist is not directly entrained into the fire but is instead first carried by the air to the side walls and is then dragged along these walls to the floor. Water-mist is then entrained into the fire along with the air flow. The temperature iso-surfaces indicate that the fire bends toward the front wall (the wall containing the door).

Figure 3 shows the iso-surfaces of the water-mist sectional density in the fire compartment 10 seconds after water-mist was injected through the nozzles. The high sectional density contours are centered around the location of the nozzles. Numerical simulations indicate that the individual nozzles are not equally effective in suppressing the fire. Water-mist from nozzles close to the door seem to evaporate earlier, whereas that from nozzles further from the door takes longer to evaporate. This is a direct consequence of the fact that the fire bends towards the front wall containing the doorway. Figure 4 shows the instantaneous streaklines originating from the fire at $t = 10\ s$ after mist injection. The streaklines have been color coded with red showing the highest temperature and blue showing the lowest temperature. The edges of the fire compartment, fine mesh in the burner and the flow of hot gases through the door are also shown. The streakline pattern illustrates that large scale vortical structures are continuously evolving in the fire compartment and are convecting through the computational domain. As new vortical structures continuously evolve and flow through the door, the flow field through the door is continuously changing. We also observe that the flow field is not symmetric on either side of the door. This is also observed in the unsymmetrical pattern of the water-mist sectional density iso-surface as seen in Figure 3.

Figure 5 through Figure 9 are numerical results of a time dependent simulation showing the effect of water-mist on the suppression of a fire. As discussed earlier, the fire was ignited at $t = 0\ s$ and was allowed to develop fully until $t = 1800\ s$. This result was then used as an initial condition for the water mist suppression studies. The time counter was reset to $t = 0\ s$. Then water-mist was injected through the nozzles at a time $t = 10\ s$. Figure 5 through 9 show temperature iso-surfaces in the fire compartment. The temperature iso-surfaces on the left represent the case without water-mist and the temperature iso-surfaces on the right represent the case with water-mist. Similarly the maximum temperature in the fire compartment for the case without water-mist injection is shown on the left and that for the case with water-mist is shown on the right. The maximum temperature can occur at any point in the computational domain and is a function of time. Since water-mist is injected after ten *seconds* the two cases are exactly identical for the first ten *seconds* of the simulation. The maximum temperature as a function of time are also exactly identical for the first 10 seconds (Figure 5).

As soon as water-mist is injected through the nozzles ($t = 10\ s$), we observe small differences in the temperature contours. As the water-mist is injected, it immediately starts interacting with the hot gases in the fire compartment. Some of the water-mist evaporates, resulting in local cooling of the flow field. The water-mist also influences the gaseous flow field due to the interphase drag force. We do not see a marked difference in the maximum temperature for the two cases. As more water-mist is injected and as time passes, the maximum temperature shows a small decrease and the temperature iso-surfaces for the two cases are different (Figure 6). At $t = 15\ s$ (Figure 7) we observe that the maximum temperature has reduced by approximately 200 degrees. We also observe that water-mist has convected along the side walls and has entrained into the fire along

Case	*Water Mist Characteristics of each nozzle*			*Total flow rate*	*Time for*
	Density (gm/cm^3)	*Velocity* (cm/s)	*Diameter*(μm)	(kg/s)	*Suppression* (sec)
T1	0.2	50.0	100	100.0	30.5
T2	0.4	50.0	100	200.0	28.0
T3	0.2	100.0	100	200.0	16.9
T4	0.4	100.0	100	400.0	10.0
T5	0.2	20.0	100	40.0	> 50.0
T6	0.2	50.0	200	100.0	35.0
T7	0.4	50.0	200	200.0	32.2
T8	0.2	100.0	200	200.0	18.4
T9	0.4	100.0	200	400.0	16.9

Table 1. Parametric studies for Top Injection Configuration. For each case four water mist nozzles were located in the ceiling.

with the air flow resulting in suppression close to the burner. There is significant suppression in the region covered by the fine mesh.

For time $t = 16$ through $t = 19$ s, progressive cooling of the fire is seen. As more and more water-mist is injected through the nozzles, we observe only isolated regions of high temperature (Figure 8) and correspondingly the maximum temperature also continuously decreases. The fire appears to be completely extinguished by time $t = 30$ s (Figure 9). At this time, the maximum temperature throughout the fire compartment is below 350 ^oK.

Efficient design of water-mist systems aims at obtaining the maximum amount of suppression for the minimum amount of water-mist added to the system. A systematic parametric study was conducted to optimize the various water-mist injection characteristics for fire suppression. The parameters that have been studied include, droplet diameter, injection density, injection velocity, nozzle location and nozzle orientation. Tables 1-4 summarize results of this parametric study. The time required for suppression (sec) as predicted in each simulation is recorded in the last column. The time for suppression is the time elapsed from the instant the water mist is injected into the fire untill the time when the peak temperature (maximum temperature) in the fire compartment is below 350 ^oK. The time for suppression does not include the time that is spent in fire detection or delivery of water to the sprinklers. Table 1 summarizes results for the top injection configuration. In the top injection configuration, four identical nozzles were located in the ceiling of the fire compartment. The nozzles are centered around the co-ordinate point $(70, 250, 70)$, $(70, 250, 170)$, $(300, 250, 70)$ and $(300, 250, 170)$ cm. Water mist is injected vertically downward with an injection velocity ranging from 50.0 cm/s to 200.0 cm/s and an injection density ranging from 0.2 gm/cm^3 to 0.4 gm/cm^3. The injected droplets are monodisperse with an initial drop diameter of 100 μm and 200 μm. For each of the nine cases listed in Table 1 for the top injection configuration, the total mist flow rate for all the four nozzles has also been shown along with the time for suppression in seconds. For the first five cases T1-T5, the drop diameter is kept fixed at 100 μm, while for cases T6-T9, the drop diameter is 200 μm.

As the injection density increases, we observe a reduction in the time for suppression. However the reduction in time for suppression is not proportional to the increase in injection density. This was observed for all injection velocities and for all droplet diameters that were tested in our study.

Case	*Water Mist Characteristics of each nozzle*			*Total flow rate*	*Time for*
	Density (gm/cm^3)	*Velocity* (cm/s)	*Diameter*(μm)	(kg/s)	*Suppression* (sec)
S1	0.2	50.0	100	100.0	78.5
S2	0.4	100.0	100	400.0	82.9
S3	0.8	100.0	100	800.0	> 100.0

Table 2. Parametric studies for Side Wall Injection Configuration. For each case two water mist nozzles were located in the two side walls.

For example, the injection density in Case T2 is twice that of Case T1, but the decrease in the time for suppression is only 2.5 s. For the larger diameter case T6 and T7 (200 μm), we again observe that the time for suppression reduces only by 2.8 s, when the injection density increases by a factor of two. A similar conclusion is reached when comparing case T8 with case T9. Our results thus indicate that the time for suppression reduces as the injection density increases, but the reduction is not proportional to the increase in injection density.

It is also observed that changing the injection velocity has a much more pronounced effect on time for suppression. Comparing case T1 and T3 we observe that the time for suppression reduces by approximately a factor of two when the injection velocity is increased by a factor of two. Comparing cases T2 and T4 we observe an even bigger reduction in time for suppression. A similar conclusion is reached when comparing case T6 with case T8 and on comparing case T7 with case T9.

Increasing the drop diameter, but maintaining a constant mist flow rate, results in an increase in the total time for suppression. Comparing case T1 with case T6 shows that the time for suppression increases by 4.5 s when the initial drop diameter is increased from 100 to 200 μm. The total flow rate is kept constant in these two cases. Similarly comparing case T3 with case T8, we observe that the time for suppression increases from 16.9 s to 18.4 s, when the drop diameter was increased from 100 to 200 μm. The total mist flow rate for Case T3 and T8 were equal to 200 kg/s. Of all the cases studied in this report, case T4 resulted in the smallest time for suppression of 10 s for a 980 kW fire.

As the water-mist is injected through the ceiling, the drag force between the gas phase and water-mist affects the movement of the water droplets and also influences the gaseous flow field. The water-mist also evaporates as it comes in contact with the hot gases resulting in smaller water droplets. The smaller diameter droplets quickly follow the gas phase and are entrained into the fire at approximately the same rate as the oxidizer. This is because the smaller droplets exhibits a small characteristic time for decrease of relative velocity between the gas and water droplets. However, larger diameter droplets tend to travel with their injection velocity and exhibit larger characteristic time for decrease in relative velocity. For the smaller droplets the drag force exerted by the gas on these droplets is able to counterbalance the droplet weight and these droplets therefore entrain into the flame along with the oxidizer. The larger droplets are not able to counterbalance the weight with the drag force.

Table 2 provides results from three cases of water-mist injection through the side walls. The two side walls are the longer edges of the fire compartment (3.7 m long). Two nozzles were located in each of the side walls. The nozzles are centered around the co-ordinate point (70, 170, 0), (70, 170, 240), (300, 170, 0) and (300, 170, 240) cm. Water mist is injected horizontally toward the

Case	*Water Mist Characteristics of each nozzle*			*Total flow rate*	*Time for*
	Density (gm/cm^3)	*Velocity* (cm/s)	*Diameter*(μm)	*(kg/s)*	*Suppression (sec)*
F1	0.2	50.0	100	100.0	> 100.0
F2	0.4	100.0	100	400.0	41.5
F3	0.8	100.0	100	800.0	> 100.0

Table 3. Parametric studies for Front and Rear Wall Injection Configuration. For each case two water mist nozzles were located in the front and rear walls.

Case	*Water Mist Characteristics of each nozzle*			*Total flow rate*	*Time for*
	Density (gm/cm^3)	*Velocity* (cm/s)	*Diameter*(μm)	*(kg/s)*	*Suppression (sec)*
B1	0.2	50.0	100	100.0	> 100.0
B2	0.4	100.0	100	400.0	> 100.0
B3	0.8	200.0	100	1600.0	> 100.0
B4	1.6	200.0	100	3200.0	> 100.0

Table 4. Parametric studies for Base Injection Configuration. For each case four water mist nozzles were located in the floor.

fire with an injection velocity ranging from 50.0 cm/s to 200.0 cm/s and an injection density ranging from 0.2 gm/cm^3 to 0.4 gm/cm^3. The injected droplets are monodisperse with an initial drop diameter of 100 μm.

Our results indicate that the time for suppression is significantly larger than the corresponding case of the Top injection configuration. Comparing cases T1 and S1, we find that the time for suppression increase from 30.5 s for the top injection configuration to 78.5 s for the side wall injection configuration. Similarly comparing cases T4 and S2, we find that the time for suppression for the side wall injection configuration is considerably larger. For case S3, we could not obtain suppression during the 100 s for which the simulation was conducted. For the side injection configuration, we also observe that the time for suppression increases with increasing values of mist flow rate. In general the side injection configuration was found to be a less efficient suppression technique than the top injection configuration.

Table 3 provides results from three cases of water-mist injection through the front and rear walls. The front and rear walls are the smaller edges of the fire compartment (2.5 m long). Two nozzles were located in each of the front and rear walls. The nozzles are centered around the co-ordinate point $(0, 170, 50)$, $(0, 170, 190)$, $(370, 170, 50)$ and $(370, 170, 190)$ cm. Water mist is injected horizontally toward the fire with an injection velocity ranging from 50.0 cm/s to 200.0 cm/s and an injection density ranging from 0.2 gm/cm^3 to 0.4 gm/cm^3. The injected droplets are monodisperse with an initial drop diameter of 100 μm and 200 μm. Water-mist injection through the front and rear walls is observed to be less efficient than the top injection configuration. Cases F1 and F3 did not result in complete fire suppression during the 100 s simulation time.

Table 4 provides results from four cases of water-mist injection through the floor. The nozzles are centered around the co-ordinate point $(50, 0, 70)$, $(50, 0, 170)$, $(300, 0, 70)$ and $(300, 0, 170)$ cm. Water mist is injected vertically upward toward the fire with an injection velocity ranging from 50.0 cm/s to 200.0 cm/s and an injection density ranging from 0.2 gm/cm^3 to 0.4 gm/cm^3. The injected droplets are monodisperse with an initial drop diameter of 100 μm and 200 μm. It appears

that the base injection configuration is the least efficient method for suppressing the fire. For all cases that were tested, complete extinction could not be obtained during the 100 s time interval.

The results of our parametric study clearly indicate that the top injection configuration results in the smallest time for suppression as compared to the other injection configurations (Side injection, Injection through the front and rear walls and Base Injection). At first glance, this result appears to contradict our earlier water-mist suppression work on small scale methane-air diffusion flames [6], [7] and liquid methanol pool fires [8], [15]. In reference [7], [15] we had shown through a detailed parametric study that the base injection configuration was the optimum injection configuration. Under base injection configuration the water-mist to fuel flow rate ratio required for extinguishment reduces with decreasing droplet size [8]. Flame suppression was observed to increase with higher injection density or lower mist velocity for a given flow rate and droplet diameter. In contrast with base injection configuration, side injection configuration [6] showed that larger diameter droplets produce more flame suppression. Under side injection configuration flame suppression increases with smaller mist density or higher injection velocity for a given flow rate and droplet diameter [6].

We had also reported in reference [6] that, under top injection configuration, the droplets were unable to overcome the drag force exerted by the hot plume gases. The droplets were observed to quickly reverse their flow direction and convect out of the computational domain along with the gas flow. If the initial injection velocity for the water droplets was very high, then the gaseous flow field was reversed resulting in propagation of acoustic waves that disturbed the flame structure. It was concluded that "Class 1" droplet sprays will be unable to penetrate through the plume region and reach the diffusion flame. Droplets that were injected away from the plume region were also unable to flow against the cooler co-flowing air. Only under the conditions of zero co-flow air velocity, were the droplets able to travel downwards under the force of gravity and able to cool the flame surface.

There are several reasons for the apparent differences in conclusions obtained from our present large scale work and our earlier work on small scale flames. One of the main reasons is that in our present work, fire simulations have been performed in an enclosed compartment, while our earlier work was in a 2-D open geometry. The enclosed compartment geometry results in a flow field that is significantly different from the flow field in the 2-D open geometry. In the present work, we observe a flow-field that is continuously evolving in time as new vortical structures are generated in the fire and convect along the ceiling and the side walls. Also as the plume hits the ceiling, it breaks up into smaller vortical structures that are observed in the fire compartment. The presence of the door further complicates the flow field as hot gases leave through the upper half of the door and cooler air is entrained into the fire through the lower half. The flow field is also unsymmetrical and is inherently 3-D in nature. In contrast, our earlier work on small scale fires exhibits a 2-D, symmetrical flow, in which cool gases enter the computational domain through one edge, undergo combustion and exit at the outflow boundary. The remaining two edges were treated as a slip wall or a line of symmetry. The flow fields in the two cases are completely different, which results in a different pattern of entrainment of the water-mist into the fire and subsequent suppression.

Also, in our earlier small scale water-mist suppression work, water-mist was injected uniformly along the entire inflow boundary in the base injection configuration along with the air flow. Water-mist that was injected very close to the flame could easily entrain into the flame and provide maximum suppression. On the other hand, water-mist that was injected far away from the flame, flowed out of the computational domain along with the air co-flow, without evaporating. In our present work with fires in large compartments, water-mist was injected at specific coordinate points

that were far away from the fire. Water-mist that is injected far from the fire in the base injection configuration, does not entrain as readily into the fire. This conclusion was obtained even in our small scale suppression work, where water-mist injected far away from the fire, flowed out of the computational domain without evaporating. Thus, the location of the nozzles plays a very critical role in determining the level of entrainment and overall fire suppression.

Finally, in our present work with water-mist injection through the ceiling (top injection configuration), we find that the nozzles are located such that the hot ceiling jet can be cooled quickly and easily in this configuration. The remaining water-mist then is entrained along with the air flow into the fire, resulting in further suppression and extinction. Thus, our results support our earlier conclusion on the dynamics of interaction between the water-mist and the fire.

4. WORK IN PROGRESS

The results of this numerical study will be compared with experimental data on water-mist suppression in single uncluttered compartments.

More detailed simulations will be pursued to model the fire growth and spread in complex ship geometries. Ultimately, simulation of full scale tests of water-mist systems will be conducted in a cluttered machinery space of the ex-USS SHADWELL. These tests will demonstrate the potential ability of water-mist to extinguish both shielded and unshielded fires in full scale, relatively cluttered machinery space applications. Several changes will be made to the present algorithms to simulate machinery spaces. These include improvements to the fire model as well as adding details to the interior of the compartments using the virtual cell embedding (VCE) technique [30].

5. ACKNOWLEDGEMENT

The work described in this report was performed by the Laboratory for Computational Physics and Fluid Dynamics of the Materials Science and Component Technology Directorate, Naval Research Laboratory. The work was funded by the Office of Naval Research, Code 334, under the Damage Control Task of the FY-00 BA2 Surface Ship Hull, Mechanical and Electrical Technology Program (PE0602121N) and the NRL 6.1 Computational Physics Task Area.

6. REFERENCES

1. Drysdale, D., *An Introduction to Fire Dynamics*, John Wiley & Sons, New York, 1985.
2. Rashbash, D.J., " The Extinction of Fire with Plain Water: A Review," Fire Safety Science, 1986, pp. 1145-1163.
3. Tatem, P.A., Beyler, C.L., DiNenno, P.J., Budnick, E.K., Back, G.G. and Younis, S.E., "A Review of Water Mist Technology for Fire Suppression," NRL/MR/6180-94-7624, Naval Research Laboratory, 1994.
4. Prasad, K., Li, C., Kailasanath, K., Ndubizu, C., Gopal, R. and Tatem, P.A.,*Numerical Modeling of Fire Suppression Using Water Mist. 1. Gaseous Methane-Air Diffusion Flame*, Naval Research Laboratory, Memorandum Rep ort, NRL/MR/6410-98-8102 (1998).
5. Prasad, K., Li, C., Kailasanath, K., Ndubizu, C., Gopal, R. and Tatem, P.A., *Numerical Modeling of Water Mist Suppression of Methane-Air Diffusion Flame*, Comb. Sci. & Tech., V. 132, 1-6, p-325 (1998).
6. Prasad, K., Li, C. and Kailasanath, K., *Numerical Modeling of Fire Suppression Using Water Mist. 2. An Optimization Study on Jet Diffusion Flames*, Naval Research Laboratory, Memorandum Report, NRL/MR/6410-98-8159 (1998).
7. Prasad, K., Li, C. and Kailasanath, K., "Optimizing Water-Mist Injection Characteristics for Suppression of Co-Flow Diffusion Flames," 27^{th} Symposium (Int.) on Combustion, pp. 2847-2855, 1998.
8. Prasad, K., Li, C., Kailasanath, K., Ndubizu, C., Gopal, R. and Tatem, P.A., *Numerical Modeling of Fire Suppression Using Water Mist. 3. Methanol Liquid Pool Fire Model*, Naval Research Laboratory, Memorandum Report, NRL/MR/6410-98-8190 (1998).
9. Prasad, K., Li, C. and Kailasanath, K., *Numerical Modeling of Fire Suppression Using Water-Mist 4. Suppression of Liquid Methanol Pool Fires,* Naval Research Laboratory, Memorandum Report, NRL/MR/6410-98-8303 (1998).
10. Prasad, K., Patnaik, G. and Kailasanath, K., *Advanced Simulation Tool for Improved Damage Assessment 1. A Multiblock Technique for Simulating Fire and Smoke Spread in Large Complex Enclosures*, Naval Research Laboratory, Memorandum Report, NRL/MR/6410-00-8428 (2000).
11. Downie, B., Polymeropoulos C. and Gogos, G., "Interaction of a Water Mist with a Buoyant Methane Diffusion Flame," Fire Safety Journal, 24, 19 95, pp. 359-381.
12. Mawhinney, J. R., "The Role of Fire Dynamics in Design of Water-Mist Fire Suppression Systems," INTERFLAM 96, 1996.
13. Mawhinney, J. R., "A Closer Look at the Fire Extinguishing Properties of Water-Mist," 4th International Symposium on Fire Safety Science, 1994.
14. Ndubizu, C., Ananth, R., Tatem, P. A., "The Effects of Droplet Size and Injection Orientation on Water Mist Suppression of Low and High Boiling Point Liquid Pool Fires," Combust. Sci and Tech, Vol. 157, pp. 63-86, 2000.
15. Prasad, K., Li, C. and Kailasanath, K., "Simulation of Water-mist Suppression of Small Scale Methanol Liquid Pool Fires," Fire Safety Journal, 33, pp. 185-212 (1999).
16. Prasad, K., Li, C., Kailasanath, K., Ndubizu, C., Ananth, R. and Tatem, P. A., "Numerical Modeling of Methanol Liquid Pool Fires," Combust. Theory Modelling, 3, 743-768 (1999).

17. Walton, W. D. and Budnick, E. K., "Quick Response Sprinklers in Office Configurations : Fire Test Results," NBS 752, 1988.

18. Cooper, L. Y. and Stroup, D. W., "Test Results and Predictions for the Response of Near-Ceiling Sprinkler Links in a Full-Scale Compartment Fire," NBS 240, 1987.

19. Alpert, R., "Calculated Interaction of Spray with Large Scale Buoyant Flows," J. Heat Transfer, 105, p. 310 (1984).

20. Bill, R. G., "Numerical Simulation of Actual Delivered Density (ADD) Measurements," Fire Safety J., 20, p. 227 (1993).

21. Mell, W.E., Baum, H.R. and McGratten, K., "Simulation of Fires with Radiative Heat Transfer," 2nd International Conference on Fire Research and Engineering, August 1997.

22. McGratten, K. and Stroup, D., "Sprinkler, Vent and Draft Curtain Interaction - Experiment and Computer Simulation," 2nd International Conference on Fire Research and Engineering, August 1997.

23. Nam, S., "Parametric Study with a Computational Model Simulating Interaction Between Fire Plume and Sprinkler Spray," Annual Conference on Fire Research, 1996.

24. Hoffman, N., Galea, E. R. and Markatos, N. C., "A Computer Simulation of Fire-Sprinkler Interaction: A Two-Phase Phenomena," 12th IMACS World Congress, Paris (1988).

25. Galea, E. R. and Markatos, N. C., "Aircraft Cabin Fires: A Numerical Simulation," 12th IMACS World Congress, Paris (1988).

26. Steger, J. L., Dougherty, F. C. and Benek, J. A., "A Chimera Grid Scheme," in *Advances in Grid Generation*, ASME FED-Vol. 5, 1983.

27. Patnaik, G., Guirguis, R. H., Boris, J. P. and Oran, E. S., "A Barely Implicit Correction for Flux-Corrected Transport", J. Comput. Phys., 71:1-20, 1987.

28. Boris, J. P. and Book, D. L., "Flux Corrected Transport I. SHASTA, A Fluid Transport Algorithm That Works,", Journal of Computational Physics, 11 (1) pp. 38-69 (1973).

29. Dembsey, N.A., Pagni, P. J. and Williamson, R. B., "Compartment Fire Experiments: Comparison with Models," Fire Safety Journal, 25 (1995), p.187-227.

30. Landsberg, A. M. and Boris, J. P., "The Virtual Cell Embedding Gridding Method: A Simple Approach for Complex Geometries," AIAA Paper No. 97-1982, 1997.

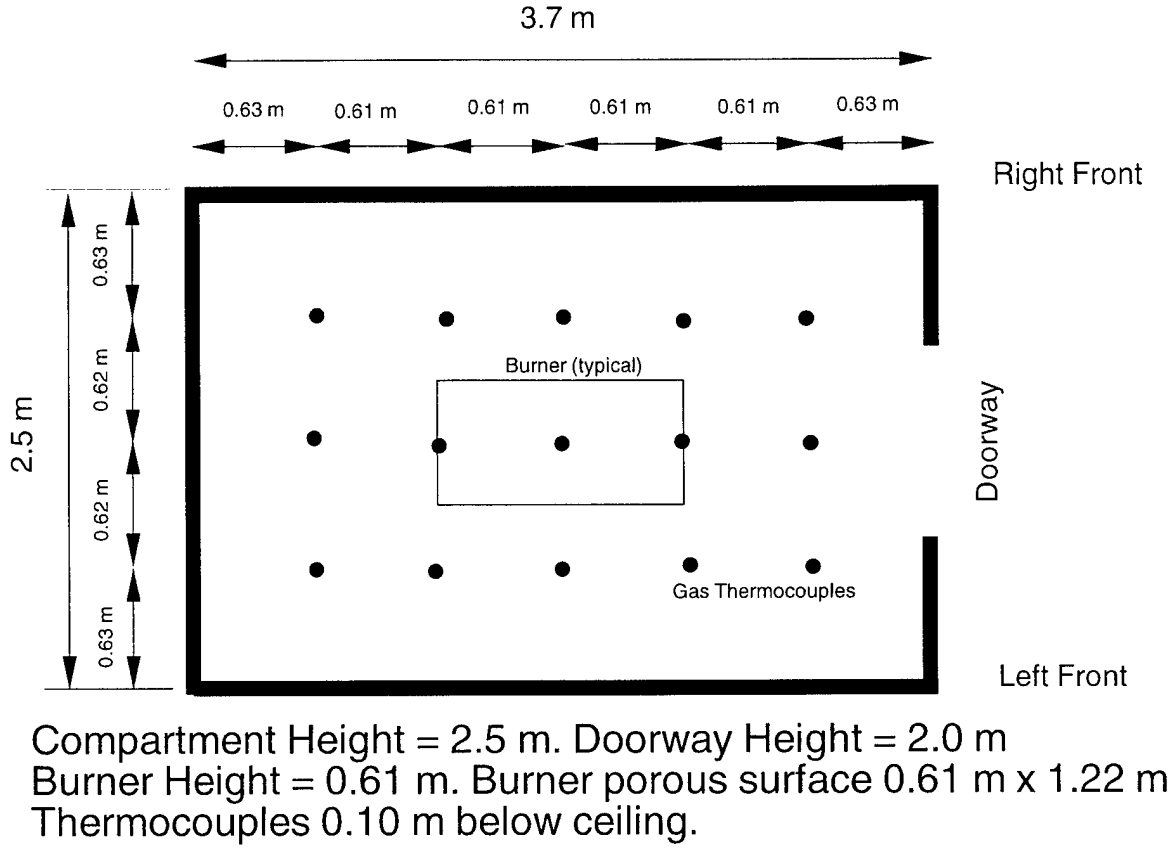

Fig. 1. Fire test compartment plan view (Reference [23]) showing locations of the ceiling gas thermocouples, the burner (located in the center of the compartment) and the doorway.

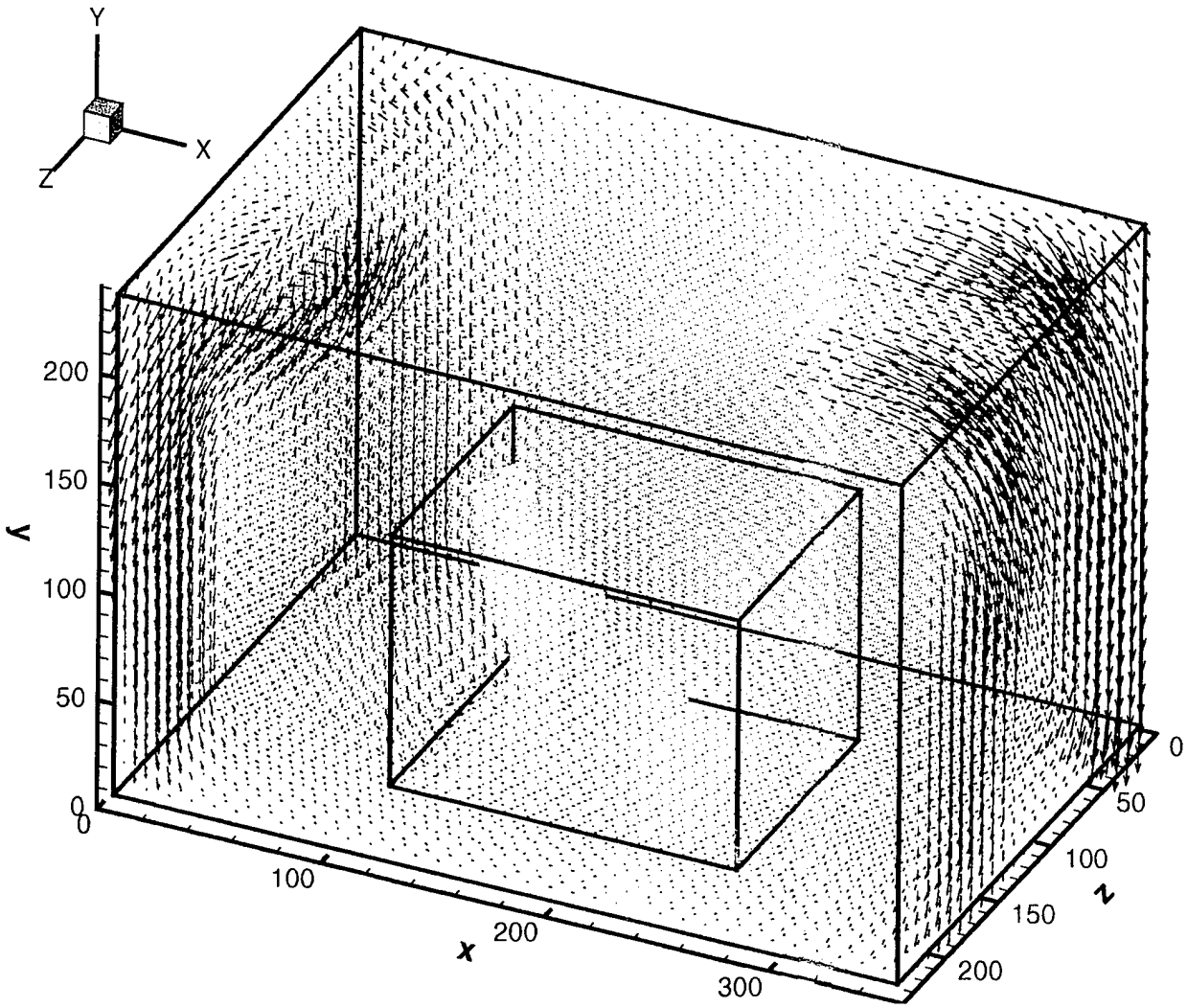

Fig. 2. Water-mist sectional velocity vectors superimposed on a 980 kW fire. The length of the arrows indicates a magnitude of the velocity vectors and the vectors point in the direction of the mist flow.

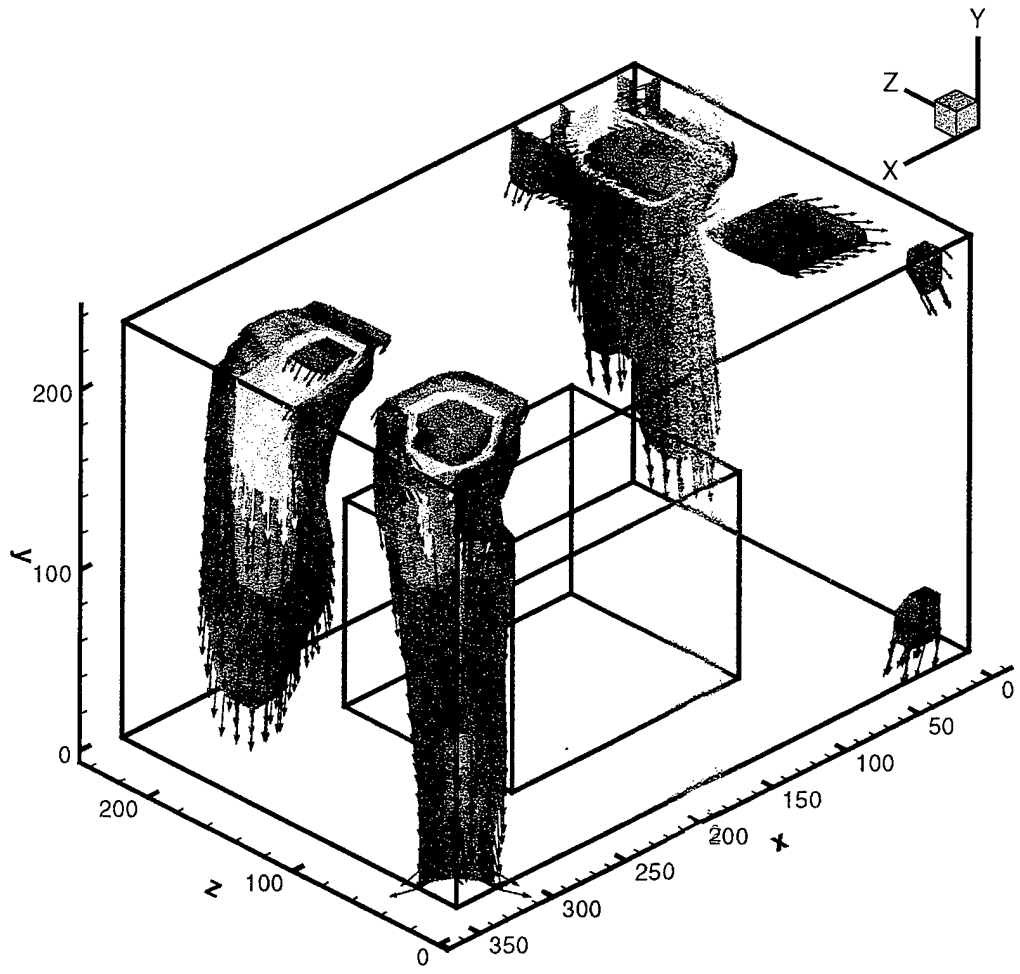

Fig. 3. Water-mist sectional density contours at 10 seconds after water-mist is injected through the nozzles. Superimposed on the density contours are the local instantaneous gas velocity vectors inside the fire compartment.

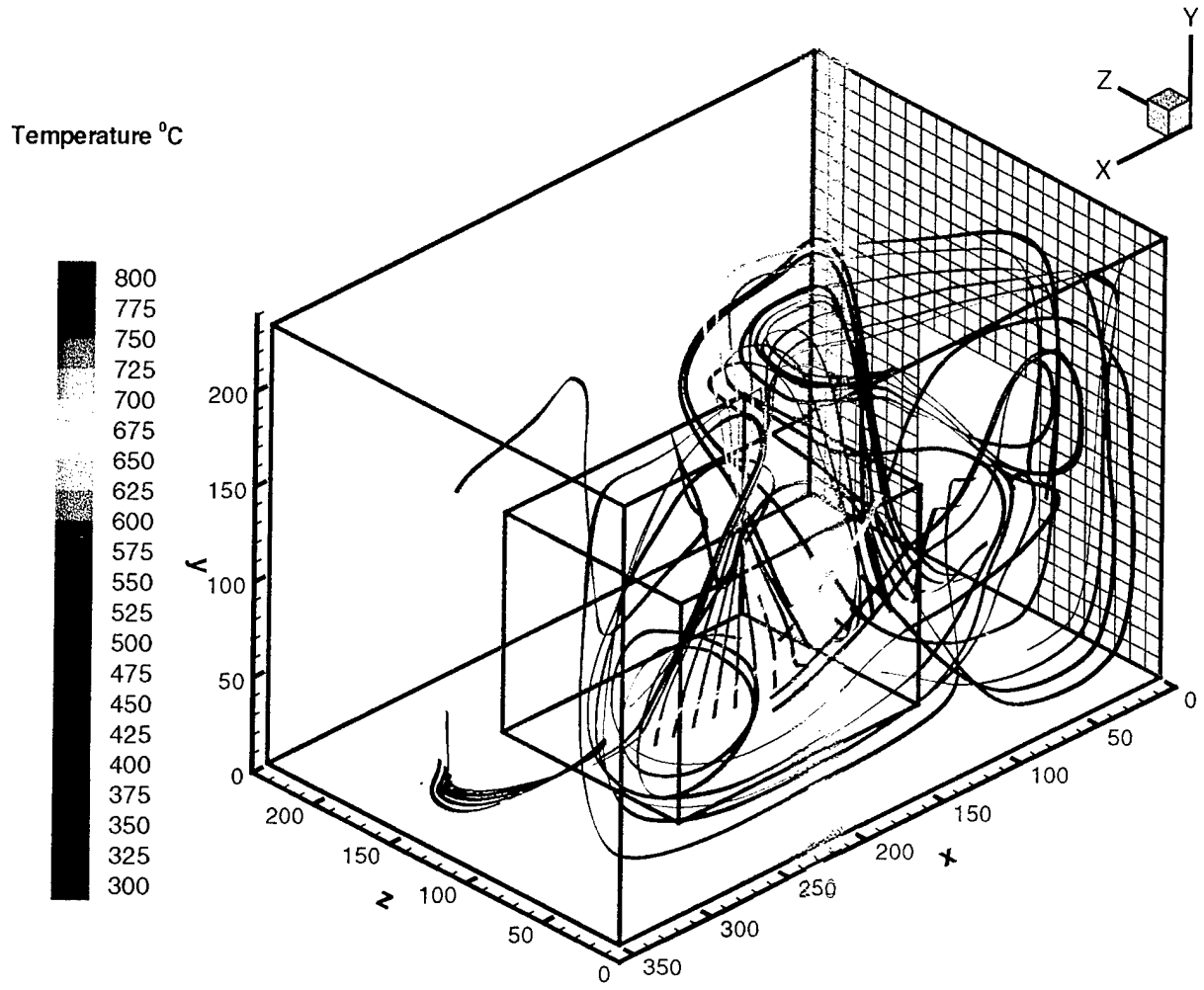

Fig. 4. Instantaneous streakline pattern originating from the fire, at a time $t = 10\ s$ after water-mist is injected through the nozzles. The streaklines have been color coded with red showing the highest temperature and blue showing the lowest temperature. The edges of the fire compartment, fine mesh in the burner and the flow of hot gases through the door are also shown.

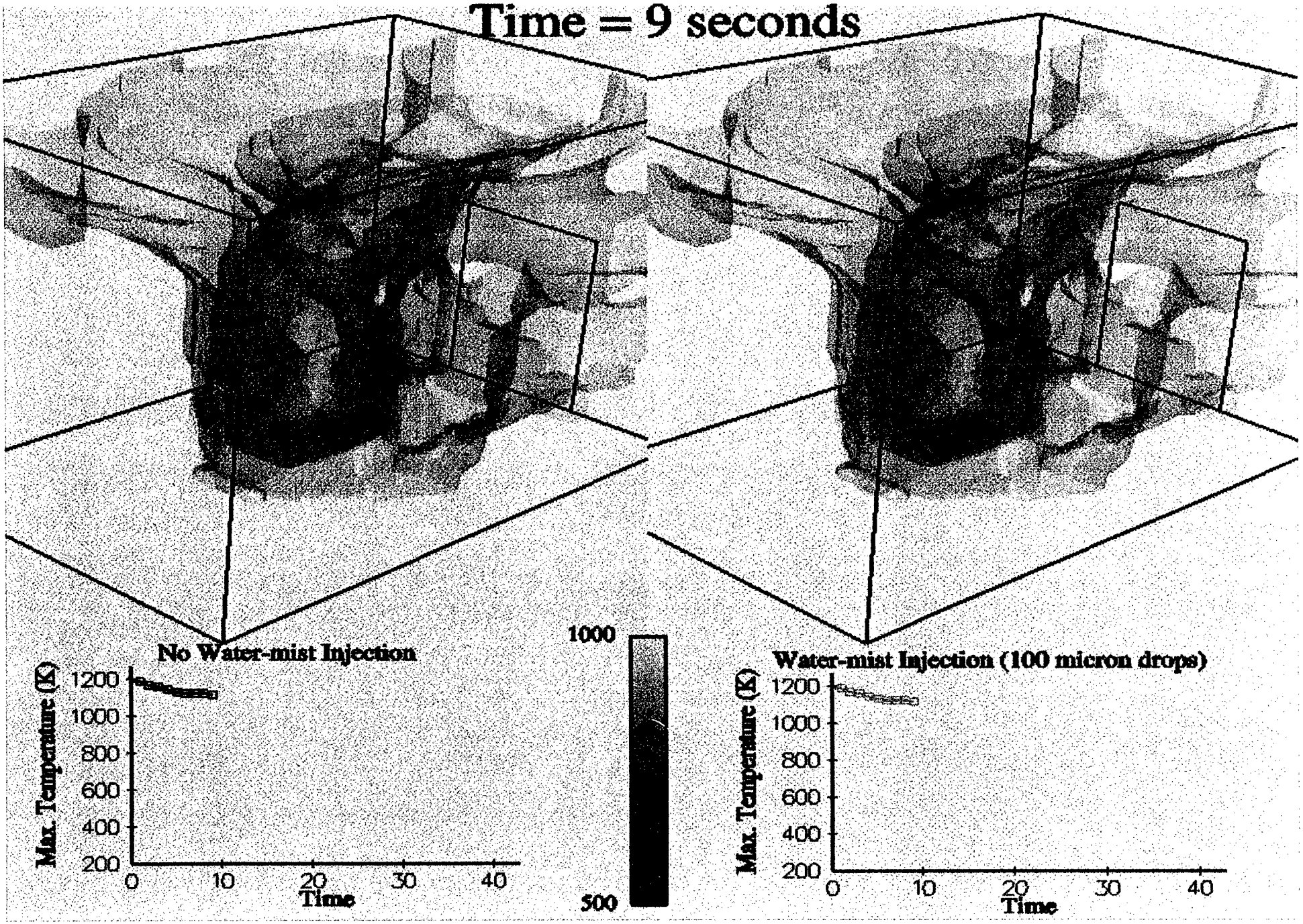

Figure 5. Comparison of two compartment fire experiments. Case without water mist injection (left) and with water mist injection (right) at t= 9 seconds.

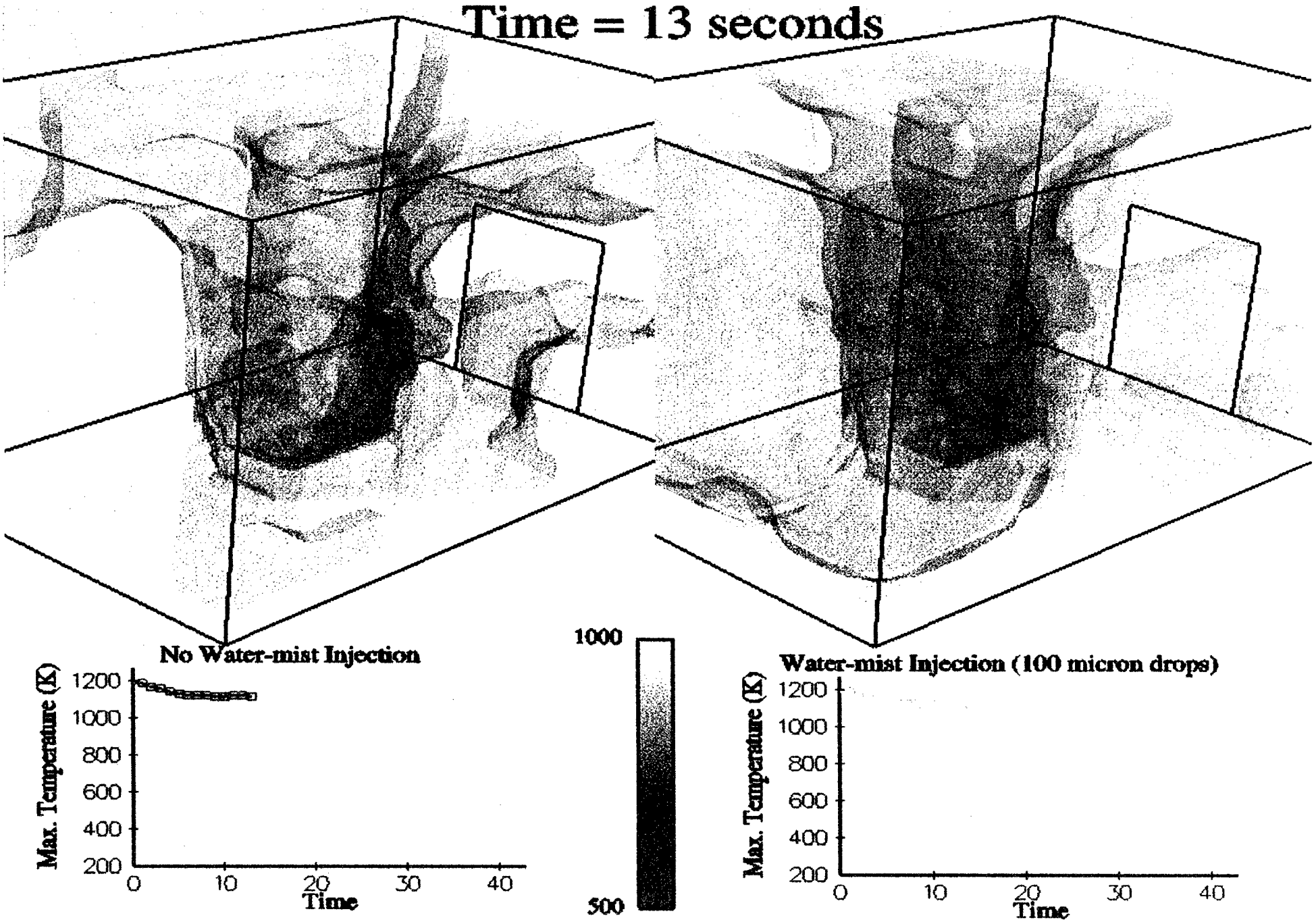

Figure 6. Comparison of two compartment fire experiments. Case without water mist injection (left) and with water mist injection (right) at t = 13 seconds.

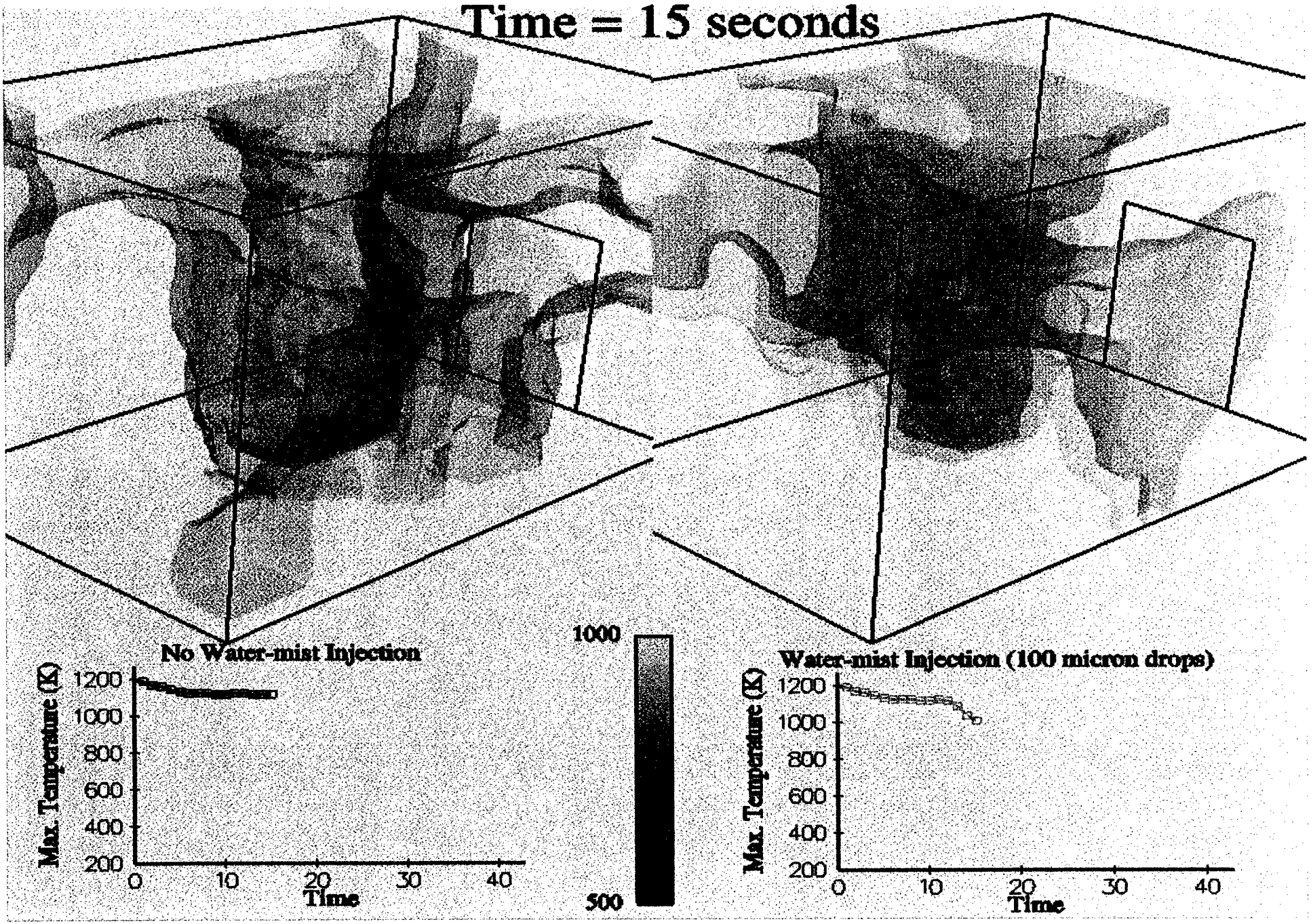

Figure 7. Comparison of two compartment fire experiments. Case without water mist injection (left) and with water mist injection (right) at t = 15 seconds.

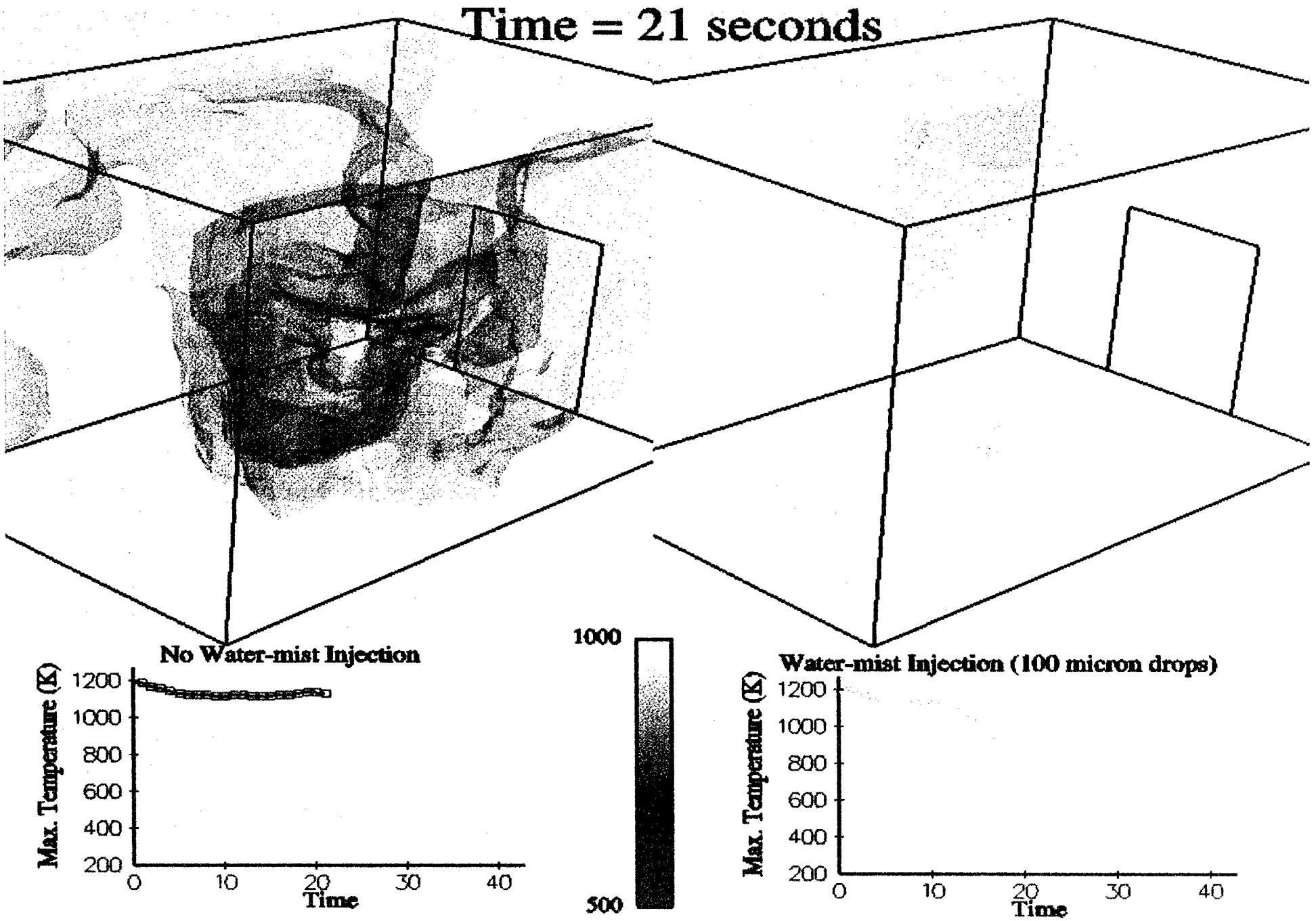

Figure 8. Comparison of two compartment fire experiments. Case without water mist injection (left) and with water mist injection (right) at t = 21 seconds.

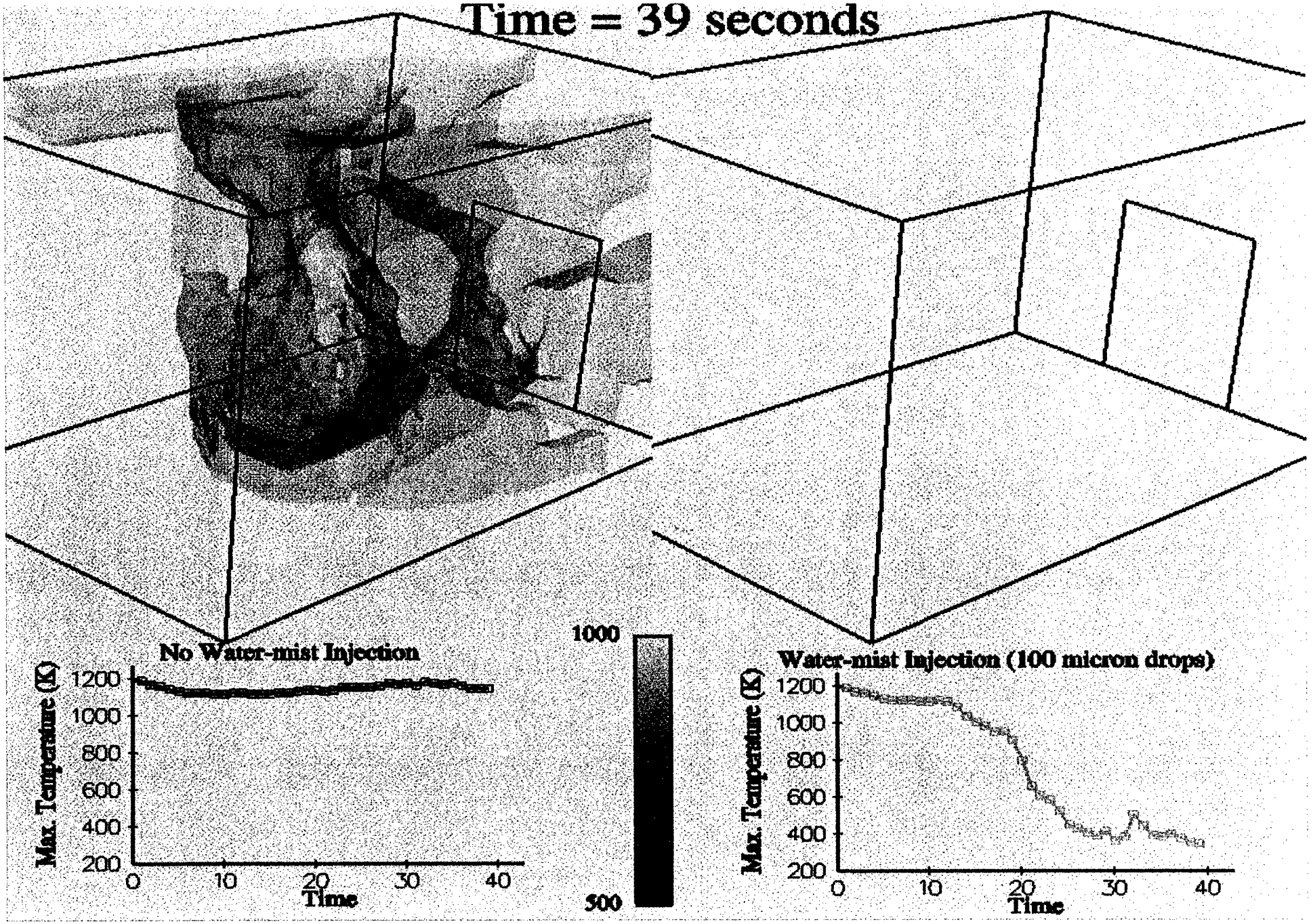

Figure 9. Comparison of two compartment fire experiments. Case without water mist injection (left) and with water mist injection (right) at t = 39 seconds.